Title

Atomic Layer Deposition of Platinum Catalysts on Nanowire Surfaces for Photoelectrochemical Water Reduction

Journal

Journal of the American Chemical Society, 135(35)

ISSN

0002-7863

Authors

Dasgupta, Neil P
Liu, Chong
Andrews, Sean
et al.

Publication Date

2013-09-04

DOI

10.1021/ja405680p

Peer reviewed

Atomic Layer Deposition of Platinum Catalysts on Nanowire Surfaces for Photoelectrochemical Water Reduction

Neil P. Dasgupta[1‡], Chong Liu[1,2‡], Sean Andrews[1,2], Fritz B. Prinz[3] and Peidong Yang*[1,2,4]

[1]Department of Chemistry, and [2]Department of Materials Science and Engineering, University of California, Berkeley, CA 94720, United States

[3]Department of Mechanical Engineering, Stanford University, Stanford, CA 94305, United States

[4]Materials Science Division, Lawrence Berkeley National Laboratory, Berkeley, CA 94720, United States

Supporting Information Placeholder

ABSTRACT: The photocathodic hydrogen evolution reaction (HER) from *p*-type Si nanowire arrays was evaluated using platinum deposited by atomic layer deposition (ALD) as a HER co-catalyst. ALD of Pt on the NW surface led to a highly conformal coating of nanoparticles with sizes ranging from 0.5-3 nm, allowing for a precise control of Pt loading in deep sub-monolayer quantities. Catalytic performance was measured using as little as 1 cycle of ALD Pt, which corresponded to a surface mass loading of ~10 ng/cm^2. The quantitative exploration reported here for the lower limits of Pt co-catalyst loading, and its application to high-surface area nanowire photoelectrodes, establish a general approach to minimize the cost of precious metal co-catalysts for efficient and affordable solar-to-fuel applications.

Due to the intermittent nature of the solar resource, energy storage technologies are a critical component of a future renewable energy infrastructure. One attractive strategy is the direct storage of solar energy in the form of chemical bonds in a process known as artificial photosynthesis[1]. While the direct splitting of water can be achieved by a single wide bandgap semiconductor, the overall thermodynamic efficiency of these systems is limited by insufficient light absorption[2]. To address this issue, a dual-bandgap system can be utilized[3], in which the electrochemical half-reactions are separated into a semiconductor photoanode and photocathode, allowing for the use of lower bandgap materials which can absorb a greater portion of the solar spectrum.

One of the issues during this solar-to-fuel process is the sluggish kinetics of the hydrogen evolution reaction (HER) at the semiconductor surface, which requires the incorporation of a co-catalyst material on the surface to reduce the reaction overpotential[4]. Among the various co-catalyst materials, noble-metals such as Pt have been shown to provide the highest electrochemical activity towards the HER. However, the high cost of precious metal co-catalysts limits the economic viability of an artificial photosynthesis scheme. While alternate co-catalyst materials based on earth-abundant elements are being explored to reduce the costs associated with the use of Pt[5] for solar-to-fuel applications, these materials still lag behind Pt in terms of electrochemical catalytic performance for the HER. An alternate approach to reduce the co-catalyst cost is to dramatically reduce the loading of Pt on the electrode surface, while maintaining sufficient catalytic activity for the chemical reaction.

One way to reduce the required catalytic activity for a given overpotential is the use of high surface area photoelectrodes[5a]. In particular, one dimensional semiconductor microwire and nanowire (NW) arrays are being explored for solar-to-fuel applications[6] owing to a large semiconductor/electrolyte interfacial area, in addition to other beneficial properties including enhanced light scattering and trapping[7] and efficient transport of charge carriers to the electrodes[8]. However, the ability to coat these high-aspect ratio structures with a uniform coating of co-catalyst particles remains challenging using traditional deposition techniques such as electrodeposition or physical vapor deposition[9], which can lead to a poor utilization of the expensive Pt material. Therefore, a technique is needed to uniformly coat the surface of high aspect ratio structures with precise control of the catalyst loading and size to minimize the overall raw material cost.

One technique which meets this requirement is atomic layer deposition (ALD)[10]. ALD is a modified chemical vapor deposition (CVD) technique capable of conformal coating of ultra-high aspect ratio structures with sub-nm precision in material thickness due to self-limiting surface reactions and

the separate introduction of material precursors in a cyclic manner. While many ALD processes lead to the formation of a dense thin film, certain reaction chemistries result in nucleation of isolated islands on the growth surface, which grow larger with increasing ALD cycle number and eventually coalesce into a film. This process has been explored for direct deposition of catalysts[11] and quantum dots[12] with diameters below 10-nm on nanostructured surfaces.

In this report, by using a Si NW array photocathode as a model system with large surface area, we show that ALD of Pt nanoparticles can serve as an efficient co-catalyst for photoelectrochemical water reduction utilizing as little as 1 cycle of ALD. Pt nanoparticles with diameters ranging from 0.5-3 nm form during the initial 3 ALD cycles, leading to a uniform catalyst loading along the length of NW with a sub-monolayer Pt surface density. Electrochemical and photoe

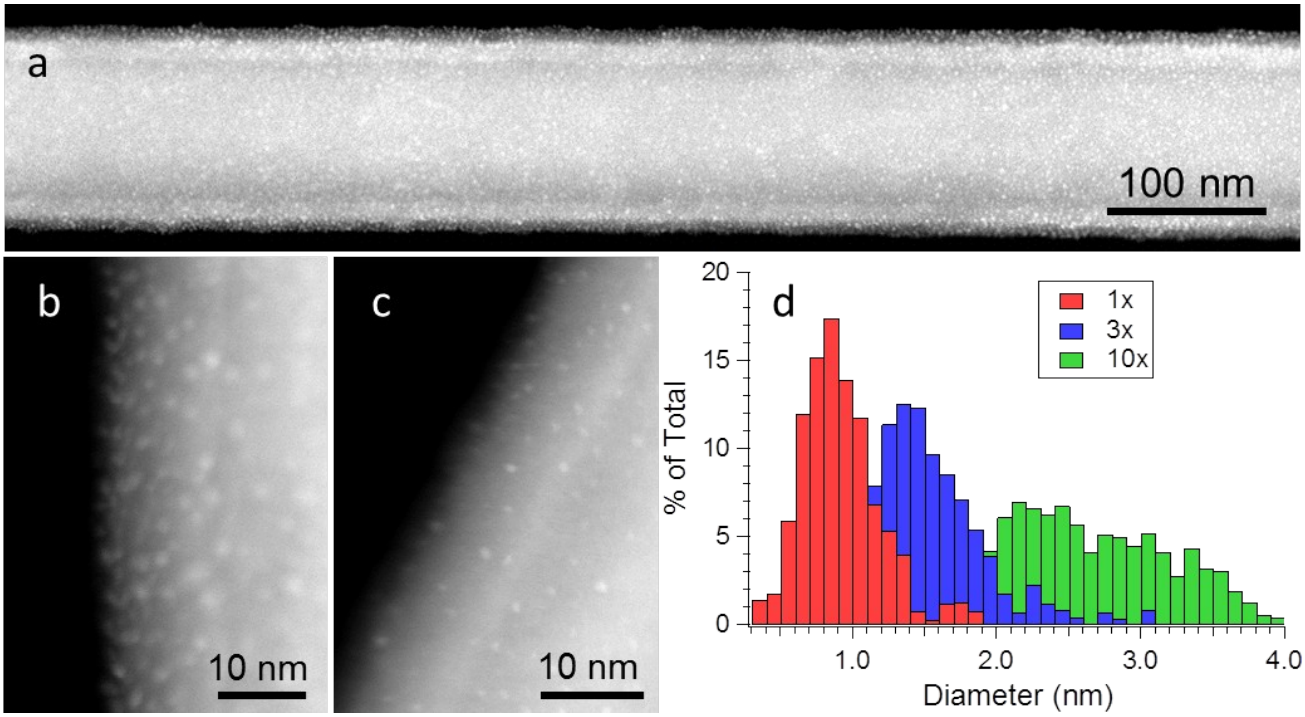

Figure 1. STEM analysis of Pt nanoparticles deposited on core-shell Si-TiO2 NWs by ALD. HAADF images of (a) 10 cycles (b) 3 cycles and (c) 1 cycle of ALD Pt. (a) Low magnification image showing a core-shell structure coated with a uniform coverage of discrete Pt nanoparticles. (d) Histogram of particle size for various cycle numbers.

lectrochemical measurements demonstrate that the HER catalytic activity of these Pt clusters on high surface area nanowire photoelectrodes is stable and sufficient for solar-to-fuel applications. The combination of highly uniform coating and precise control of nanoparticle size and loading in the ALD process is a powerful tool which can take advantage of the benefits of the NW geometry while minimizing the total volume of Pt required.

P-type Si NW arrays were selected as a photocathode material due to a suitable conduction band edge with respect to the HER potential and a sufficiently low bandgap for visible light absorption[4a]. The well-defined NW arrays (Supporting information) provide a high surface area structure suitable for quantitative analysis. To achieve a positive photovoltage and stabilize the Si surface, a *p*-Si/TiO_2 core-shell structure was formed by ALD of 10-12 nm TiO_2 on the nanowire surface, which was followed by deposition of Pt by ALD[13].

The morphology of the core-shell *p*-Si/TiO_2 NWs loaded with Pt NPs was observed using aberration-corrected scanning transmission electron microscopy (STEM), as shown in Figure 1. Nucleation of sub-nm scale islands on the NW surface was observed after only 1 ALD cycle (Figure 1c). A low-magnification STEM analysis demonstrated the excellent uniformity of the ALD coatings along the length of the NW surface (Figure 1a). This was further confirmed by a high magnification STEM analysis at different regions along the length of a NW coated by 1 cycle

(Supporting information). A high resolution image of a single 2nm Pt NP shows a crystalline phase with a d-spacing of 2.3 Å (Supporting information). A histogram of the lateral dimension of the islands based on several images is shown in Figure 1d. We measure an average particle diameter of 0.8 nm after 1 cycle, with a standard deviation of 0.25 nm. The size and density of the Pt particles on the surface can be seen to increase with increasing cycle number, showing the ability to control the Pt loading and particle size by simply varying the number of ALD cycles. We note that the STEM images over-represent the absolute value of surface particle density due to the curved surface of the nanowires, and the fact that we observe nanoclusters on both sides of the nanowire in the image.

It is well known that ALD Pt exhibits a non-linear nucleation phase during the initial cycles[11c,11f,11h], which is highly dependent on the ALD conditions and surface chemistry of the substrate[14]. The exact nucleation mechanisms are still a matter of intense research[15]. The formation of clusters in this size range suggests that surface diffusion of Pt atoms occurs during the initial cycles, leading to a sparse distribution of Pt clusters on the surface, rather than a uniform monolayer of atoms. Further research into these nucleation and surface diffusion phenomena in the future is likely to improve the ability to control the size and density of the Pt clusters with greater precision.

To provide a more quantitative measure of surface coverage, total-reflection x-ray fluoresecence (TXRF) was performed on a planar Si wafer coated with the same ALD conditions (Supporting information). After 1 cycle ALD of Pt, the surface coverage was measured to be 4.0±0.5 $\times 10^{13}$ cm^{-2}, which corresponds to a surface density of about 2.7% compared to the Pt (111) surface (1.5 x 10^{15} cm^{-2}), and a platinum mass loading of approximately 10 ng/cm^2, which is consistent with the STEM analysis of the NW surface (Supporting information). Therefore, while the atomic-scale distribution of Pt atoms on the surface is not homogeneous due to the formation of Pt clusters, the co-catalyst loading via ALD is in the deep sub-monolayer level. Furthermore, from shallow-angle x-ray photoelectron spectroscopy (XPS) measurements, an increase in the peak intensity can be observed with increasing the number of ALD cycles, showing an monotonic increase in the Pt loading with increasing cycle number (Supporting information). Achieving these low levels of Pt loading uniformly over a high-aspect ratio surface would be extremely difficult by standard Pt deposition techniques, allowing us to efficiently explore the lower limits of Pt loading for catalytic activity of the HER reaction.

The electrocatalytic performance of the Pt NPs was tested using planar fluorine-doped tin oxide (FTO) substrates as an electrode (Supporting information). 12 nm of TiO_2 was first deposited on the FTO surface, followed by Pt of varying number of ALD cycles to replicate the conditions on the *p*-Si nanowires. The catalytic performance was measured using linear sweep voltammetry in 0.5M H_2SO_4 electrolyte with series resistance subtracted, under a standard three-electrode configuration. The measured onset of cathodic current for a potential negative of 0V vs. the reversible hydrogen electrode (RHE) (Figure 2a) and the observed formation of gas bubbles at high current density imply catalytic activity for the HER. With an increasing number of Pt ALD cycles the cathodic currents increase, consistent with the confirmed increase of Pt loading amount. From the Tafel plots shown in Figure 2b, all samples exhibit a current slope of about 60 mV per decade, and the apparent exchange current densities for substrates of different ALD cycles were obtained (Table 1).

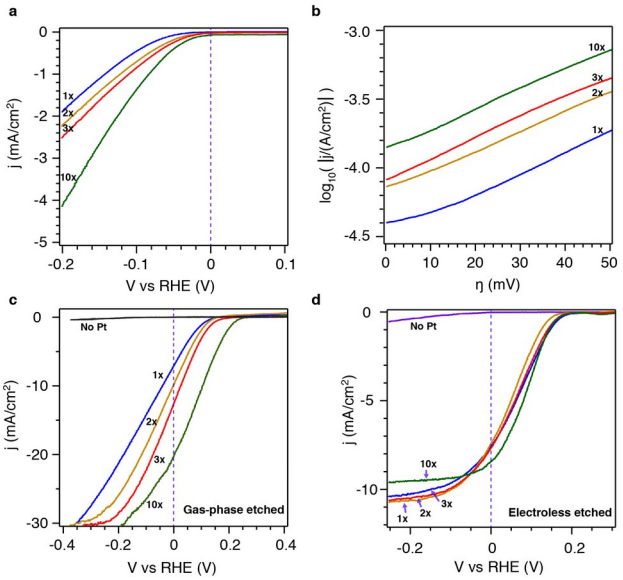

Figure 2. Electrochemical (a,b) and photoelectrochemical (c,d) performance of Pt co-catalysts loaded via ALD in 0.5M H_2SO_4 electrolyte. (a) Linear sweep voltammetry and (b) Tafel plots of ALD Pt after various cycles on FTO substrates coated with 12 nm TiO_2. (c) H_2 evolution performance of Si NW array photocathodes synthesized via gas-phase etching under 1 sun illumination, loaded with ALD Pt co-catalyst. (d) H_2 evolution performance of Si NW photocathode synthesized via electroless etching, under the same condition as (c).

In the case of high surface area structures, the required catalytic activity is reduced due to the lower actual current density on the surface. Therefore, the ability to precisely control the Pt loading in this sub-monolayer regime allows for an exploration of the lower limits of required platinum usage in high aspect-ratio structures. To test this hypothesis, the PEC performance of these Pt catalysts was tested on Si NW array photocathodes.

A well-defined large surface area Si NW array electrode was synthesized via gas-phase deep reactive ion etching (DRIE) method (Supporting infomation). The PEC performance of these photocathodes was tested under the same condition as the above electrochemical measurement. It was empirically found that the thin TiO_2 interlayer was required to achieve positive photovoltages with these ALD Pt catalysts on the Si surface. A similar phenomenon has been observed in e-beam evaporated Pt catalysts on bare Si, which was attributed to the formation of an ohmic contact

between Si and Pt, which determined the energetics of the Si-Pt-electrolyte interface[5a]. However, the presence of an intermediate TiO_2 barrier layer allowed for the observation of a characteristic photocathode *J*-V curve with as low as 1 ALD cycle, despite the ultralow Pt loading under these conditions. As shown in Figure 2c, the absence of Pt co-catalyst gives no photoactivity of the Si NW photocathode. For all samples measured, an onset voltage of 0.15-0.25 V vs. RHE and current densities of ~30 mA/cm^2 was observed under 100 mW/cm^2 simulated AM 1.5 irradiation.

Moreover, the slope of this J-V curve was seen to increase with increasing number of ALD cycles from 1 to 10, leading to an increase of the current density from 7 – 20 mA/cm^2 at 0V vs. RHE, which are comparable to previous results for *p*-Si wires using standard Pt processing techniques[5a]. This indicates that the HER catalytic activity of the Pt atoms on the NW surface determines the slope of the J-V curve. Table 1 shows a comparison of the surface loading of Pt (calculated from the TXRF and XPS data) with the electrochemical and photoelectrochemical performance of the ALD Pt catalysts (further details in the Supporting information).

Table 1. Summary of electrochemical and photoelectrochemical performance of ALD Pt catalysts

Cycles	Surface Pt loading (ng/cm^2)	j_0 (μA/cm^2)	J_{sc} @ 0V vs. RHE (mA/cm^2)
1	13±3	2.7±0.4	7.1
2	24±5	5.9±0.9	8.3
3	34±7	8.5±1.0	12.5
10	105±21	13±2	20.7

These results demonstrate the ability to tune the catalytic activity of the Pt nanoparticles based on simply varying the number of ALD cycles, while maintaining very low levels of Pt loading. For an affordable application of overall water-splitting by coupling two light-absorbing semiconductors, a current density on the order of 10 mA/cm^2 is expected[4a]. The photocathode of 1 cycle ALD Pt provides a current density about 7 mA/cm^2 at 0V vs. RHE, indicating that ALD Pt for co-catalyst loading is applicable for an affordable integrated water-splitting system.

To study the impact of NW surface area on the required catalytic activity, the ALD TiO_2/Pt coatings were deposited on electroless-etched NW arrays (synthesis in Support Info) with a higher surface roughness factor than the gas-phase etched nanowires. By increasing the surface area, the surface flux of electrons will be lower, leading to a lower requirement of catalytic activity on the surface. Due to the high surface area of these structures, the J-V behavior of the arrays (Figure 2d) did not vary significantly even when the number of ALD cycles was reduced to 1. On the other hand, the electroless-etched nanowire arrays led to a decrease in photocurrent, which could be due to increased surface recombination for these larger surface areas. Therefore, while further decreasing the NW diameter may decrease the catalyst activity and material purity requirements due to an increased surface area and decreased minority carrier diffusion length requirement, an optimization exists after which point additional surface area will begin to detrimentally affect the performance of NW array photoelectrodes.

Another important consideration for PEC energy conversion is the stability of the photoelectrode under illumination in the electrolyte solution. Si photocathodes are known to suffer from degradation under operating conditions, which is attributed to oxidation of the Si surface. Recently, thin TiO_2 layers have been shown to stabilize the Si surface against oxidation, which is due to efficient electronic transport through the TiO_2 layer[16]. The photocurrent in our core-shell NW was measured to be stable with no measureable degradation after one hour of illuminuation in solution (Supporting information), suggesting that the thin TiO_2 interfacial layer provided an additional benefit of stabilizing the semiconductor surface. Further optimization of this interfacial layer is currently being investigated, to maximize the onset voltage and stability of this system.

In this study, we have quantitatively analyzed the catalytic activity of sub-monolayer Pt NPs deposited by ALD. Catalytic activity was observed for as low as 1 cycle of ALD, corresponding to a surface coverage of approximately 4 x 10^{13} atoms/cm^2. The photoelectrochemical catalytic performance of these NPs was evaluated on NW surfaces, providing a quantitative exploration of the lower limits of Pt loading on high surface area electrodes. The ALD technique facilitates uniform coverage of high aspect ratio surfaces with these ultralow Pt loadings, which could potentially reduce the costs associated with use of noble metal catalysts. Additionally, the presence of an interfacial TiO_2 layer was found to be important to improve the photovoltage and stability of these Pt coated NW arrays.

ASSOCIATED CONTENT

Supporting Information

Experimental details, additional TEM and SEM data, stability measurement, and calculations of electrochemical performance. This material is available free of charge via the Internet at http://pubs.acs.org.

AUTHOR INFORMATION

Corresponding Author

p_yang@berkeley.edu

Author Contributions

‡These authors contributed equally.

Notes

The authors declare no competing financial interests.

ACKNOWLEDGMENT

N.P.D. acknowledges support from the U.S. Department of Energy, Office of Energy Efficiency and Renewable Energy (EERE) Postdoctoral Research Awards under the SunShot Solar Energy Technologies Program.

REFERENCES

(1) (a) Lewis, N. S.; Nocera, D. G. *Proc. Natl. Acad. Sci. U.S.A.* **2006**, *103*, 15729. (b) Listorti, A.; Durrant, J.; Barber, J. *Nature Mater.* **2009**, *8*, 929. (c) Bard, A. J.; Fox, M. A. *Acc. Chem. Res.* **1995**, *28*, 141.

(2) Bolton, J. R.; Strickler, S. J.; Connolly, J. S. *Nature* **1985**, *316*, 495.

(3) (a) Ohashi, K.; McCann, J.; Bockris, J. O. M. *Nature* **1977**, *266*, 610. (b) Nozik, A. J. *Appl. Phys. Lett.* **1976**, *29*, 150. (c) Kudo, A. *MRS Bull.* **2011**, *36*, 32.

(4) (a) Walter, M. G.; Warren, E. L.; McKone, J. R.; Boettcher, S. W.; Mi, Q.; Santori, E. A.; Lewis, N. S. *Chem. Rev.* **2010**, *110*, 6446. (b) Skúlason, E.; Tripkovic, V.; Björketun, M. E.; Gudmundsdóttir, S. d.; Karlberg, G.; Rossmeisl, J.; Bligaard, T.; Jónsson, H.; Nørskov, J. K. *J. Phys. Chem. C* **2010**, *114*, 18182.

(5) (a) McKone, J. R.; Warren, E. L.; Bierman, M. J.; Boettcher, S. W.; Brunschwig, B. S.; Lewis, N. S.; Gray, H. B. *Energy Environ. Sci.* **2011**, *4*, 3573. (b) Hou, Y.; Abrams, B. L.; Vesborg, P. C. K.; Björketun, M. E.; Herbst, K.; Bech, L.; Setti, A. M.; Damsgaard, C. D.; Pedersen, T.; Hansen, O.; Rossmeisl, J.; Dahl, S.; Nørskov, J. K.; Chorkendorff, I. *Nature Mater.* **2011**, *10*, 434. (c) Hinnemann, B.; Moses, P. G.; Bonde, J.; Jørgensen, K. P.; Nielsen, J. H.; Horch, S.; Chorkendorff, I.; Nørskov, J. K. *J. Am. Chem. Soc.* **2005**, *127*, 5308. (d) Chen, Z.; Cummins, D.; Reinecke, B. N.; Clark, E.; Sunkara, M. K.; Jaramillo, T. F. *Nano Lett.* **2011**, *11*, 4168. (e) Warren, E. L.; McKone, J. R.; Atwater, H. A.; Gray, H. B.; Lewis, N. S. *Energy Environ. Sci.* **2012**, *5*, 9653.

(6) (a) Yang, P. *MRS Bull.* **2012**, *37*, 806. (b) Boettcher, S. W.; Warren, E. L.; Putnam, M. C.; Santori, E. A.; Turner-Evans, D.; Kelzenberg, M. D.; Walter, M. G.; McKone, J. R.; Brunschwig, B. S.; Atwater, H. A.; Lewis, N. S. *J. Am. Chem. Soc.* **2011**, *133*, 1216.

(7) (a) Garnett, E.; Yang, P. *Nano Lett.* **2010**, *10*, 1082. (b) Kelzenberg, M. D.; Boettcher, S. W.; Petykiewicz, J. A.; Turner-Evans, D. B.; Putnam, M. C.; Warren, E. L.; Spurgeon, J. M.; Briggs, R. M.; Lewis, N. S.; Atwater, H. A. *Nature Mater.* **2010**, *9*, 239. (c) Hu, L.; Chen, G. *Nano Lett.* **2007**, *7*, 3249.

(8) (a) Kayes, B. M.; Atwater, H. A.; Lewis, N. S. *J. Appl. Phys.* **2005**, *97*, 114302. (b) Law, M.; Greene, L. E.; Johnson, J. C.; Saykally, R.; Yang, P. D. *Nature Mater.* **2005**, *4*, 455.

(9) Oh, I.; Kye, J.; Hwang, S. *Nano Lett.* **2011**, *12*, 298.

(10) George, S. M. *Chem. Rev.* **2009**, *110*, 111.

(11) (a) Elam, J. W.; Dasgupta, N. P.; Prinz, F. B. *MRS Bull.* **2011**, *36*, 899. (b) Liu, C.; Wang, C. C.; Kei, C. C.; Hsueh, Y. C.; Perng, T. P. *Small* **2009**, *5*, 1535. (c) King, J. S.; Wittstock, A.; Biener, J.; Kucheyev, S. O.; Wang, Y. M.; Baumann, T. F.; Giri, S. K.; Hamza, A. V.; Baeumer, M.; Bent, S. F. *Nano Lett.* **2008**, *8*, 2405. (d) Christensen, S. T.; Feng, H.; Libera, J. L.; Guo, N.; Miller, J. T.; Stair, P. C.; Elam, J. W. *Nano Lett.* **2010**, *10*, 3047. (e) Feng, H.; Elam, J. W.; Libera, J. A.; Setthapun, W.; Stair, P. C. *Chem. Mater.* **2010**, *22*, 3133. (f) Christensen, S. T.; Elam, J. W.; Rabuffetti, F. A.; Ma, Q.; Weigand, S. J.; Lee, B.; Seifert, S.; Stair, P. C.; Poeppelmeier, K. R.; Hersam, M. C.; Bedzyk, M. J. *Small* **2009**, *5*, 750. (g) Hsu, I. J.; Kimmel, Y. C.; Jiang, X.; Willis, B. G.; Chen, J. G. *Chem. Comm.* **2012**, *48*, 1063. (h) Chao, C.-C.; Motoyama, M.; Prinz, F. B. *Adv. Energy Mater.* **2012**, *2*, 651.

Table of Contents Figure

(12) Dasgupta, N. P.; Jung, H. J.; Trejo, O.; McDowell, M. T.; Hryciw, A.; Brongersma, M.; Sinclair, R.; Prinz, F. B. *Nano Lett.* **2011**, *11*, 934.

(13) Aaltonen, T.; Ritala, M.; Sajavaara, T.; Keinonen, J.; Leskela, M. *Chem. Mater.* **2003**, *15*, 1924.

(14) Lee, H. B. R.; Bent, S. F. *Chem. Mater.* **2012**, *24*, 279.

(15) (a) Aaltonen, T.; Rahtu, A.; Ritala, M.; Leskela, M. *Electrochem. Solid-State Lett.* **2003**, *6*, C130. (b) Elliott, S. D. *Langmuir* **2010**, *26*, 9179. (c) Mackus, A. J. M.; Leick, N.; Baker, L.; Kessels, W. M. M. *Chem. Mater.* **2012**, *24*, 1752.

(16) Seger, B.; Pedersen, T.; Laursen, A. B.; Vesborg, P. C. K.; Hansen, O.; Chorkendorff, I. *J. Am. Chem. Soc.* **2013**, *135*, 1057

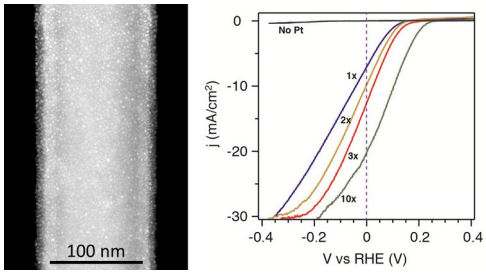
100 nm
No Pt
1x
2x
3x
10x
j (mA/cm²)
0
-10
-20
-30
-0.4
-0.2
0
0.2
0.4
V vs RHE (V)